Available online at www.sciencedirect.com
ScienceDirect
Cement and Concrete Research 37 (2007) 1248–1256
Cement and Concrete Research

Shear strength components of concrete under direct shearing

R.C.K. Wong [a,*], S.K.Y. Ma [a,1], R.H.C. Wong [b], K.T. Chau [b]

[a] Schulich School of Engineering, Department of Civil Engineering, The University of Calgary, 2500 University Drive NW, Calgary, Alberta, Canada T2N 1N4
[b] Department of Civil and Structural Engineering, Hong Kong Polytechnic University, Hong Kong, China

Received 29 July 2005; accepted 23 February 2007

Abstract

Direct shear tests on concrete specimens were conducted to investigate the shearing behaviour of the material under varying normal confining stresses. Test results were analyzed to quantify the mobilization of shear strength components derived from hydrated cement paste–aggregate adhesion, contact friction, shear dilation, and cement–aggregate interlock along the sheared surface under direct shearing. It was found that each component has its unique response in terms of mobilized shear stress and shear displacement. In addition, different modes of failure observed in uniaxial compression, splitting tension, and direct shear tests were identified to delineate the Mohr–Coulomb failure envelope for shear strength of concrete material.

Keywords: Concrete; Hydrated cement paste–aggregate bond; Shear dilation; Friction; Interlock direct shear

1. Introduction

Shear design is one of the important criteria in design of reinforced and prestressed concrete structural members. Different shear design methods have been developed depending on the shear transfer mechanism [1]. For example, in beam design compression field model is used to explain the shear transfer near support ends or in shorter beams with span-depth ratio ranging from 1 to 5. In such design cases, the compression field varies at each beam section depending on the beam span-depth ratio and loading pattern. The shear compression failure plane is controlled by the orientation of the maximum shear stress derived in the compression field. Thus, the shear failure plane is not restricted in the beam section, and could be at any inclined angle. In design cases where the sheared section is more restricted and the normal stress acting on the sheared section is more uniform than those in beams, shear transfer mechanism involves direct shearing through the initially uncracked section. For this class of problem, shear friction approach is the preferred method of solution. Practical applications of direct shearing are found in design of composite concrete beams [2], corbels [3], and offshore foundation caisson [4]. This paper focuses on shear transfer in concrete by shear friction under direct shearing.

Shear design methods based on shear friction models (e.g., [5–7]) require determination of shear strength envelope of concrete material, i.e., the relationship between the mobilized shear stress and the applied normal stress in failure. In most of previous studies, shear strength of concrete was determined from tests on reinforced concrete sections. The normal confining stress exerted at the sheared section was assumed to be equal to the forces derived from yielding of the steel reinforcements. Mast [6] used an apparent friction angle higher than the friction angle of concrete material to account for the adhesion developed in the transition zone between the hydrated cement paste (HCP) and the aggregates (referred to as HCP–aggregate transition zone adhesion herein) at normal confining stresses less than 2 MPa. At such low normal confining stresses, the principal source of adhesion is the van der Waals forces of attraction existed between the solid surfaces involved [8]. Generally, the adhesive strength in the transition zone is weaker than that in bulk HCP because water firms tend to develop around aggregates inducing a high local water-cement ratio. Hofbeck et al. [9] performed push-off tests on uncracked and cracked sections with reinforcement ratios of 0 to 2.8% or

* Corresponding author. Tel.: +1 403 220 4998; fax: +1 403 282 7026.
E-mail address: rckwong@ucalgary.ca (R.C.K. Wong).
[1] Tel.: +1 403 220 4998; fax: +1 403 282 7026.

0008-8846/$ - see front matter © 2007 Elsevier Ltd. All rights reserved.
doi:10.1016/j.cemconres.2007.02.021

equivalent normal stresses of 0 to 9.8 MPa. Their results of push-off tests are presented in Fig. 1. They observed that the ultimate shear strength of the specimens depends on the uniaxial compressive strength of concrete, reinforcement ratio or normal stress, and existence of crack. The mobilized shear strength increases with increasing compressive strength and reinforcement ratio. The initially uncracked specimens are stronger than those cracked specimens. The shear strength envelopes for uncracked and cracked specimens are non-linear particularly at normal stresses less than 2 MPa. Curve-fitting these test data shows that the test data follow consistently with the power laws as illustrated in Fig. 1. Loov [7] re-analyzed Hofbeck's test data of Fig. 1, and proposed a non-linear Mohr failure envelope for the push-off tests. In his model the shear strength is assumed to be proportional to the square root of the product of the concrete uniaxial compressive strength and the normal confining stress where the normal confining stress is derived from the yielding of the steel reinforcement. Fig. 2 shows how Loov's non-linear relationship compares with the results from the push-off tests. Based on these tests, the proportionality constant or the slope of the equation is 0.46 and 0.57 for the uncracked and cracked sections, respectively. Loov's equation provides good correlation on the cracked section, but yields underestimation on the uncracked section because the power law does not consider the effect of the adhesive strength derived in the HCP–aggregate transition zone at unconfined condition.

Paulay and Loeber [10] were apparently the first to study the shear transfer mechanism by aggregate interlock in concrete. Walraven [11] developed a statistical model simulating the cement–aggregate interlock. The derived equations were substantiated by push-off tests on cracked reinforced concrete specimens [12,13].

Recently, Sonnenberg et al. [14] conducted direct shear tests on uncracked and pre-cracked concrete specimens. The uniaxial compressive strength of the tested concrete specimens lies in a range of 26 to 42 MPa. They found that the shear strength follows a bi-linear Mohr–Coulomb failure envelope. They explained that the change in gradient point on the bi-linear envelope was attributed to the failure mode changing from the cleavage sliding failure at low normal stress to a shear failure at high normal stress. Their test results show that the direct shear capacity is proportional to the uniaxial compressive strength of the concrete. This response is consistent with Loov's equation.

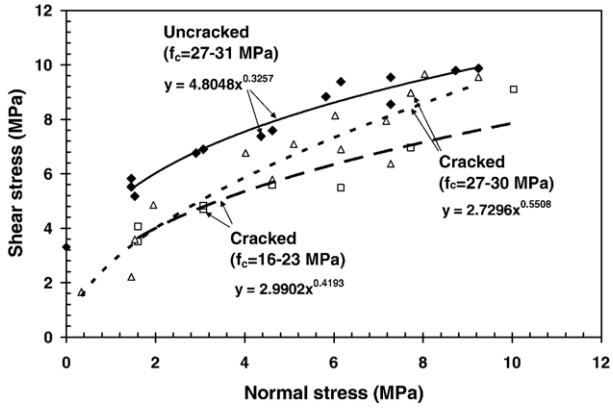

Fig. 1. Results of push-off tests from [9] (f_c=uniaxial compressive strength of concrete).

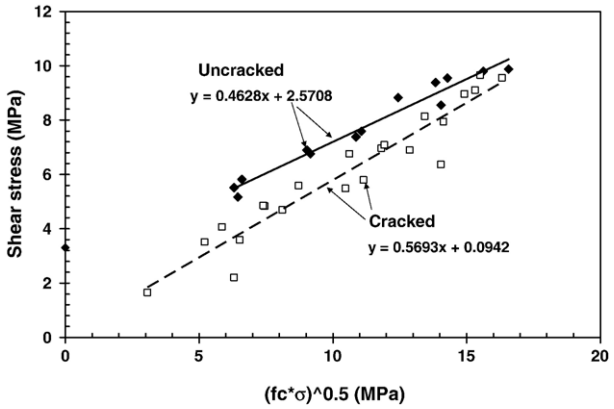

Fig. 2. Shear failure envelope proposed by Loov [7] (f_c=uniaxial compressive strength of concrete; σ=confining stress).

Other advanced shear friction models (e.g., [15–17]) adopt theories of plasticity to account for the non-linear deformation of concrete material occurred at states close to yielding or ultimate strength. This type of models requires full description of the stress–strain relationship which is defined by complex functions of yield criterion and plastic potential with appropriate flow rule.

One of the major limitations in the previous studies is that the shear strength envelope is determined by curve-fitting the data at the ultimate or peak state. In addition, no information on the deformation mode and shear strength mobilization is given. The shear strength envelopes shown in Figs. 1 and 2 are referred to as the total shear strength mobilized at the ultimate or peak state. It is of practical importance, particularly for serviceability state design, to identify all potential components contributing to the total shear strength of the concrete material. They include HCP–aggregate transition zone adhesion, friction, shear dilation, and cement–aggregate interlock along the sheared surface. In addition, it is important to quantify how each component is mobilized with increasing shear displacement.

This Paper aims at the objective of studying the shear behaviour of concrete material at varying normal stress subjected to direct shearing. The first part of the Paper describes the experimental work including uniaxial compression, indirect tensile, and shear box tests. The second part presents the experimental results. Finally, the experimental data are analyzed and presented to illustrate mobilization of various shear strength components at varying normal stresses from the initially unstressed state to the ultimate failure.

2. Experimental technique

2.1. Material

The concrete specimens used in this study were made of water, Portland cement, sand and crushed granite (10–20 mm) as coarse aggregate. The designed 28-day compressive strength

was about 40 MPa. The proportions of the designed mix are shown in Table 1.

The coarse aggregates were added to a concrete mixer followed by sand, cement, and water. The mixture was allowed to blend thoroughly for about 10 min to achieve a homogeneous state. Then, the concrete mixture was poured into molds mounted on a vibrating table. The cast was allowed to vibrate for about 5 min to reduce the air pores inside the mixture. The specimens were cured at room temperature for one day for initial setting. Then, the specimens were removed from the molds and cured in water for 28 days. The above procedures were applied to preparation of specimens for all tests including uniaxial compression, indirect tensile, and shear box tests.

2.2. Uniaxial compressive strength (UCS) tests

Cylindrical metal molds of dimensions of 100 × 200 mm were used for concrete specimens for uniaxial compressive strength tests. The end surfaces of the specimens were smoothened within +/− 0.025 mm using a grinding machine according to ASTM D2938-95 [18]. Two 66 mm TML polyester strain gauges, available from Senorcraft Technology, were mounted to the specimen using P-2 adhesive. The vertically and horizontally mounted strain gauges were used to measure the axial and radial deformations of the specimen, respectively.

The uniaxial compressive strength tests were carried out using Wykeham Farrance WF-55623 loading machine. A loading rate of 5 kN/min was used for all UCS tests. Data including axial load, axial and radial deformations were collected.

2.3. Indirect tensile strength tests (Brazilian tests)

For indirect tensile strength tests, cylindrical specimens of 100 mm in length and 60 mm in diameter, respectively were cast. Then, the cylindrical specimens were cut into cores of 30 mm in thickness according to ASTM C496-86 [18]. A loading rate of 0.5 kN/min was applied to the test core gradually until the occurrence of the first tensile crack developed across the loaded diameter was observed. The maximum applied load was recorded using a data logger.

2.4. Direct shear tests

Direct shear tests are commonly used in determination of shear strength of soil and rock in geotechnical testing. Fig. 3 shows the basic configuration of the apparatus. The apparatus consists of an upper and lower half boxes inside which the test specimen is mounted. A displacement controlled motor or pump is used to drive the upper half moving horizontally relative to the bottom half while a constant vertical normal force is applied to the top of the shear box. During the shearing, forces and displacements in horizontal and vertical directions are monitored continually.

Table 1
Designed mix of concrete

Content	Proportion
Cement (kg/m^3)	300
Water (kg/m^3)	180 (w/c = 0.6)
Sand (kg/m^3)	663
Aggregates (kg/m^3)	354

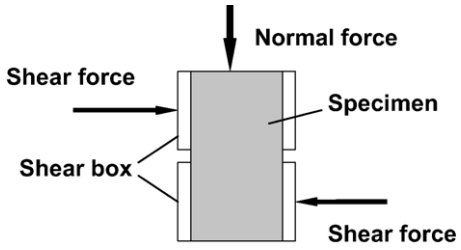

Fig. 3. Basic configuration of direct shear test.

Rectangular metal molds of dimensions of 140 × 140 × 300 mm were used to cast the concrete specimens for the direct shear tests. After curing, the specimen was positioned at the center of the lower half of the direct shear box apparatus as shown in Fig. 4a. The direct shear box was made up of two halves, lower and upper. The dimensions of each half were 200 × B200 × 160 mm. The walls of the box were made of metal with a thickness of 20 mm. The two halves were secured together by a front cover and handle. A grouting mixture made of water and plaster with an ultimate

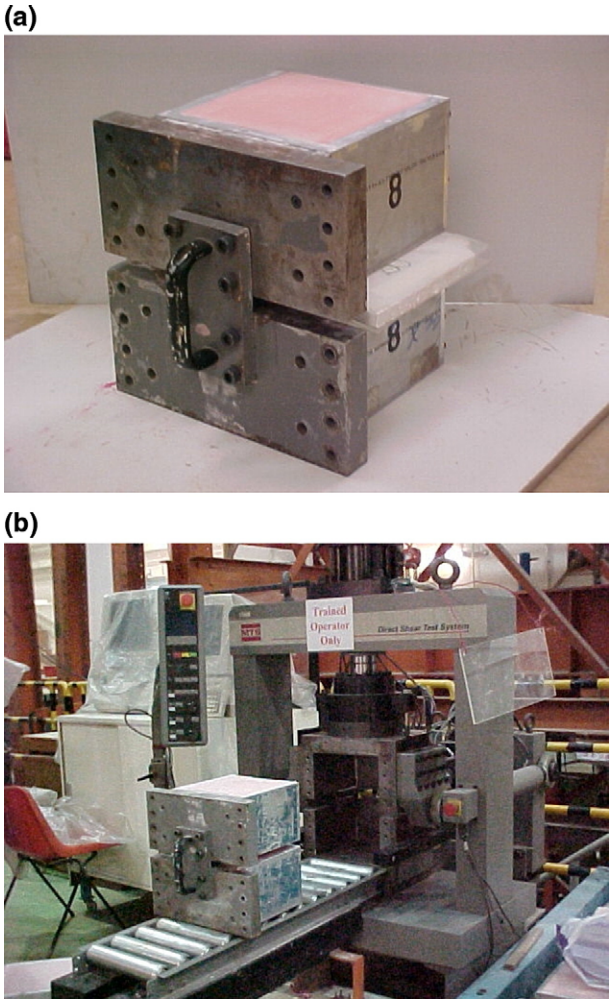

Fig. 4. (a) Specimen preparation for direct shear test (b) setup detail of direct shear test.

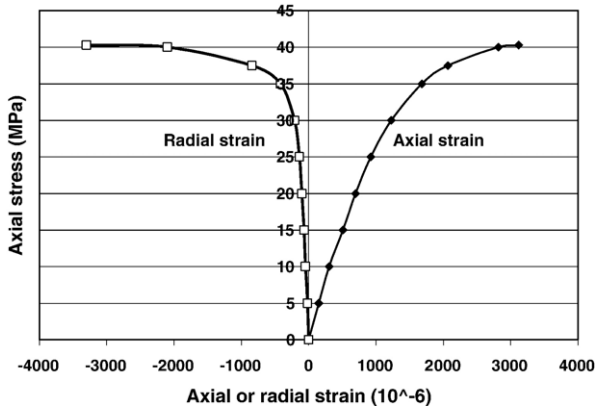

Fig. 5. Axial stress versus axial and radial strains (uniaxial compression test).

strength of 80 MPa was poured into the lower half to secure the specimen inside the box. Then, the upper half was assembled to the lower half by the front cover and handle. Dividers made of 20-mm thick Styrofoam were used to fill the gap between the upper and lower halves. Then, another batch of grouting mixture was poured into the upper half, and allowed to cure inside at room temperature for 7 days to achieve the ultimate strength prior to direct shear testing.

After 7 days of curing, the Styrofoam divider was removed, and the shear box was positioned inside the servo-controlled MTS Direct Shear Machine (Fig. 4b). The machine is capable of applying a maximum load of 261 kN in normal (vertical) and shear (horizontal) directions. Then, a designated normal load was applied to the upper half of the shear box, and the specimen was sheared at a rate of 0.05 mm/min until failure.

3. Data collection and analysis

3.1. Uniaxial compressive strength tests

Fig. 5 shows the stress–strain response of a concrete specimen loaded up to failure in uniaxial compression. The specimen exhibited a linear response with a slope of 28.6 GPa when it was loaded up to 50% of the ultimate strength. The Poisson's ratio for this linear response is about 0.16. The specimen shows some non-linearity at an axial strain of about 0.07% or 50% of the ultimate strength indicating occurrence of some plastic deformation. The specimen fails at an ultimate compressive strength of 40.4 MPa, at an average overall axial strain of 0.3%. The entire specimen shows a compressive volumetric strain initially until the axial strain reaches 0.15% where the shear dilation (dilative volumetric strain) initiates (Fig. 6). The dilation continues to persist until failure.

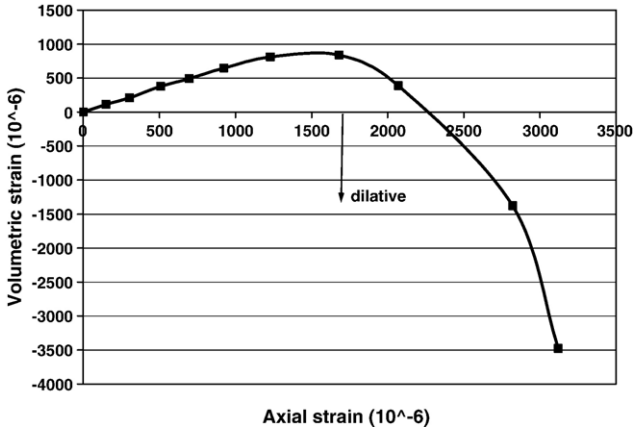

Fig. 6. Plot of volumetric strain versus axial strain showing the dilation (uniaxial compression test).

Table 2
Physical and mechanical properties of concrete specimens determined from uniaxial compressive strength tests

Sample no.	Density (kg/m3)	Uniaxial compressive strength (MPa)	Young's modulus (GPa)	Poisson's ratio
UCS01	2330	40.33	28.7	0.16
UCS02	2338	42.49	28.7	0.16
UCS03	2334	41.17	27.9	0.16

Table 2 summarizes some physical and mechanical properties of three concrete specimens in this test series.

3.2. Indirect tensile strength tests

Table 3 presents the values of tensile strength determined indirectly from three Brazilian tests. They lie in a range of 4.85–7.54 MPa, about 11.5–18.7% of UCS. These values are higher than those predicted by Mirza et al. [19]. According to their statistical analysis of relationship between splitting tensile and uniaxial compressive strength, the tensile strength of concrete generally falls in between 8 and 15% of the compressive strength.

3.3. Direct shear tests

Fig. 7 presents the results of three direct shear tests on concrete specimens under normal stresses of 3, 4.4, and 6 MPa, respectively. Fig. 7a shows that the initial portion of the shear stress–shear displacement is linear up to about 30 to 40% of the peak shear strength. The normal stress has no observable effect on the shear stiffness of the concrete specimens because of rigid plastic stress–strain relationships of bulk cement and aggregate. The peak strength occurs at a shear displacement of about 1.5–2.0 mm. The normal stress delays the occurrence of the peak strength, which indicates some degree of friction mobilization at the peak. After the peak, three specimens exhibit severe weakening, and the shear strength decreases in a constant rate. From the plot of vertical displacement versus horizontal displacement (Fig. 7b), three specimens show a small initial shear compression followed by a shear dilation. The shear

Table 3
Physical and mechanical properties of concrete specimens determined from splitting tensile (Brazilian) tests

Sample no.	Density (kg/m3)	Indirect tensile strength (MPa)
BC01	2267	7.54
BC02	2267	4.85
BC03	2267	4.92

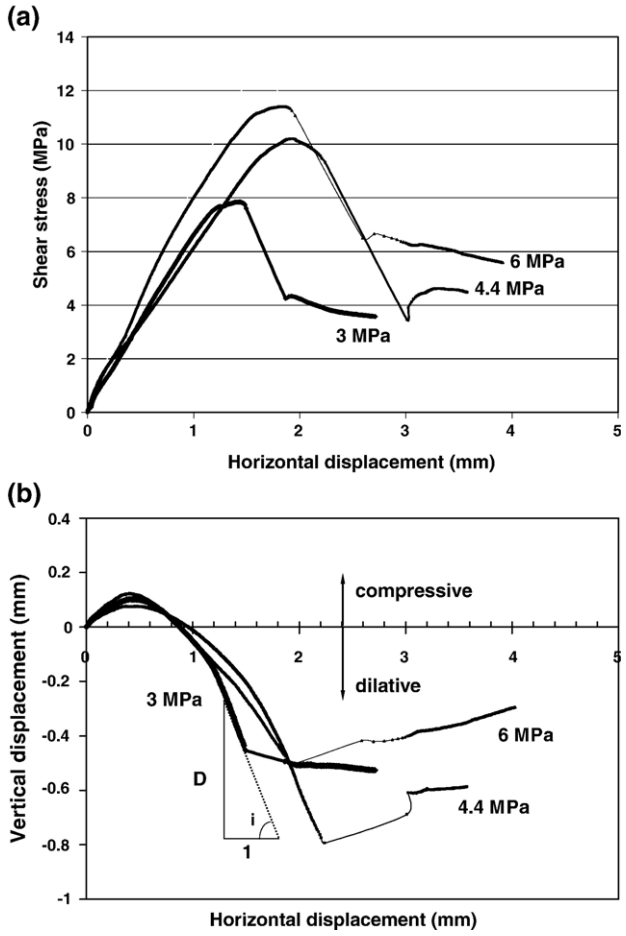

Fig. 7. Plots of (a) shear stress versus horizontal displacement and (b) vertical displacement versus horizontal displacement for direct shear tests at normal stresses of 3, 4.4 and 6 MPa.

dilation initiation occurs at a horizontal shear displacement about 0.4–0.5 mm. The dilation rate (D), defined as the ratio of the vertical displacement increment to the horizontal one or the slope of the curve (Fig. 7b), increases thereafter, and reaches a maximum value which coincides with the occurrence of the peak strength. After the peak, the dilation rate decreases drastically with increasing shear displacement. Comparison among three direct shear tests results indicates that the shear displacement for peak strength mobilization increases with increasing normal stress and the maximum dilation rate decreases with increasing normal stress. The responses of the three direct shear tests shown in Fig. 7 are consistent with those observed in 38 direct shear tests by Sonnenberg et al. [14].

4. Analysis of shear strength components in concrete under direct shearing

Concrete material contains air voids of various size and shape in bulk HCP and at the transition zone between the HCP and aggregates. Under direct shearing, no cracks are initiated at the tips of air voids up to about 50% of the failure shear stress [8]. At this state, a stable system of micro-cracks exists in the vicinity of aggregates. Upon increasing shear stress, cracks are initiated within the bulk HCP and the HCP–aggregate transition zone. The crack number and size increases with increasing shear stress level. The cracks in the bulk HCP and the transition zone eventually coalesce forming a continuous fracture through the specimen. Shear dilation (crack dilation) occurs thereafter if the imposed contact stress does not exceed the strength capacities of HCP and aggregate. For normal strength concrete (<60 MPa) in which the stiffness and strength of aggregates are much greater than those of HCP, shear transfer through the sheared fracture is dominated by the cement–aggregate interlock [11]. The interlock mechanism is characterized with sliding at the contact area between the HCP and aggregates at the opposite sides of the crack and cement crushing at contacts. For high strength concrete (100 MPa), the HCP is sufficiently strong to cause aggregate crushing destroying the interlocked structure [13].

In summary, the total shear strength of concrete specimens measured in direct shear tests is a combination of effects from the HCP–aggregate transition zone adhesion, contact friction, shear dilation, and cement–aggregate interlock along the sheared fractured surface.

4.1. Contact friction

According to Coulomb's law of friction, the limiting static friction force is directly proportional to the resultant normal

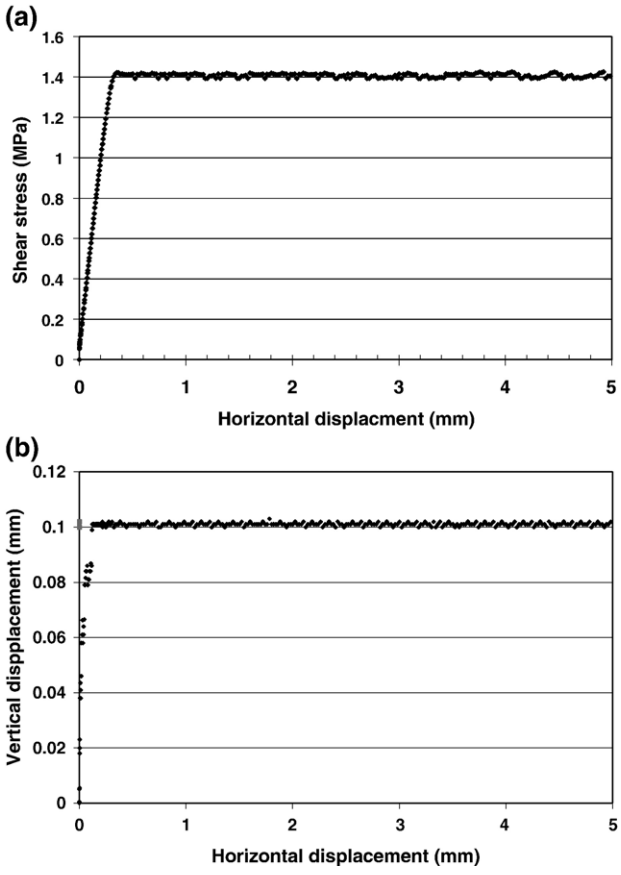

Fig. 8. (a) Mobilized friction (b) vertical displacement versus horizontal displacement along a concrete plane in a direct shear test at normal stress of 2.8 MPa.

force applied to the contact surface. The constant of proportionality is defined as the coefficient of static friction or tan(ϕ) where ϕ is the friction angle of the material at the contact. Concrete is made up of cement, sand, and aggregate. The coefficient of friction of concrete is a function of those of these solid materials. A control direct shear test was conducted to determine the coefficient of static friction on the concrete material used. Fig. 8 shows the results from this control test in which two concrete blocks were sheared along a smooth contact surface in the direct shear box. The smooth contact surface was prepared by the grinding method similar to the one used in preparing the end surfaces of the cylindrical concrete specimens for the uniaxial compressive strength tests. The control test eliminates the shear resistance derived from the effect of surface roughness, and provides direct measurement of the intrinsic static friction. From Fig. 8a, the shear strength derived from friction is under a normal stress of 2.8 MPa, yielding a coefficient of static friction of 0.51 or friction angle (ϕ) of 27°. The full mobilization of shear friction requires a shear displacement of about 0.35–0.40 mm. No shear compression or dilation was observed during the friction mobilization indicating the shear plane was horizontal with respect to the horizontal shear stress applied. The static friction coefficients reported in literature were determined based on back analysis on test results of sheared concrete specimen. The reported values lie in a range of 0.4 to 0.6 [11,20].

4.2. Shear dilation

Walraven's cement–aggregate interlock model [11] assumes shearing at a constant crack width without considering the effect of shear or crack dilation. Effect of shear dilation on shear strength enhancement in dense sand was well presented in [21]. Fig. 9 illustrates the effect of shear dilation on the shear stress measured in the direct shear test. On this figure, an upper block is displaced along a shear plane with an inclined angle, i. Based on the force equilibrium equations, the following relationship can be obtained:

$$\frac{F_s}{F_n} = \tan(\phi + i) \tag{1}$$

where

F_s horizontal shear force;
F_n vertical normal force;

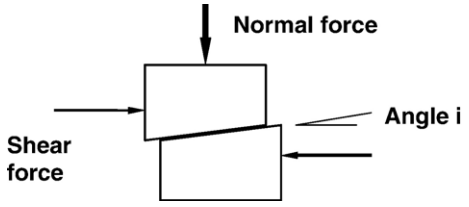

Fig. 9. Shear dilation model.

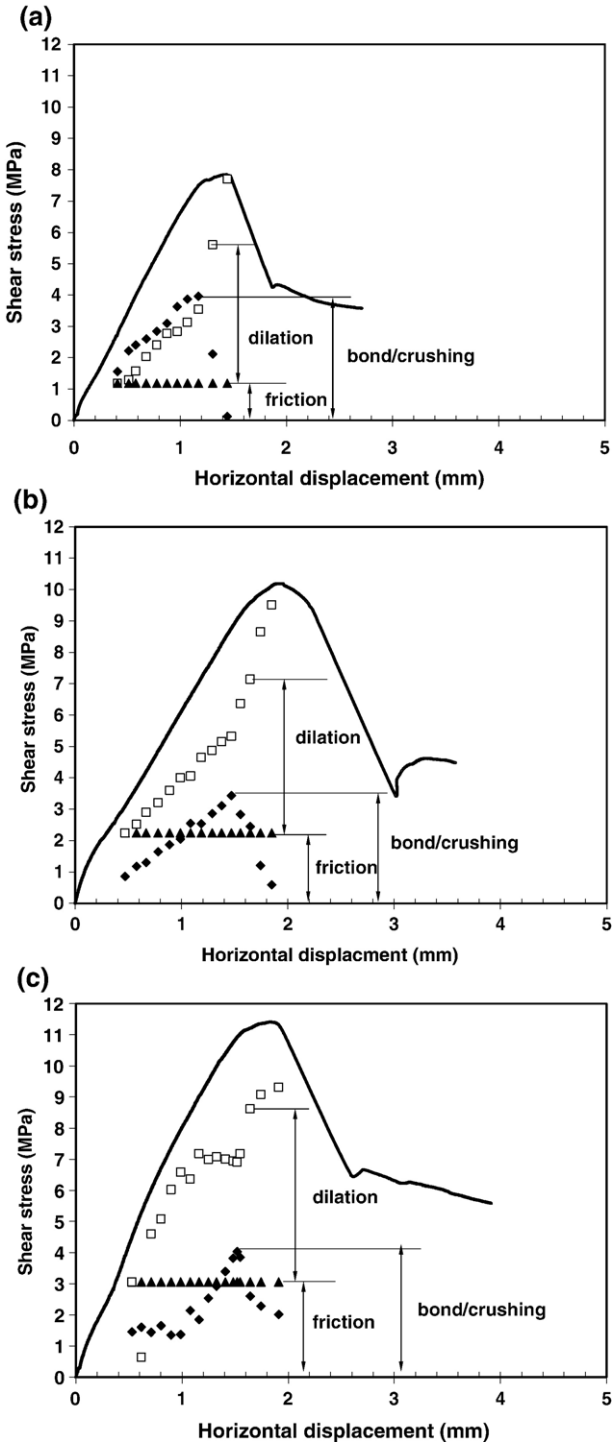

Fig. 10. Mobilized shear strength components for direct shear tests at normal stresses of (a) 3 MPa (b) 4.4 MPa and (c) 6 MPa.

ϕ intrinsic friction angle corresponding to the coefficient of static friction;
i dilation angle ($i=\tan^{-1}(D)$ where D=shear dilation rate as defined in Fig. 7b.

For $i=0$, no vertical displacement (shear dilation) will be detected during shearing. The upper block will start to move if the

horizontal force applied reaches the friction force. The horizontal force normalized with the normal contact force is equal to the coefficient of static friction or tan(ϕ). A positive upward angle i will induce a vertical displacement or shear dilation. The horizontal–vertical displacement increment, D measured in the direct shear tests reflects this angle i or shear dilation rate. The horizontal force required for such an upward displacement is greater than that for $i = 0$. Thus, the measured horizontal force in such case of $i > 0$ is an indication of the friction property and shear dilation defined by ϕ and i, respectively.

4.3. HCP–aggregate transition zone adhesion and cement–aggregate interlock

Based on the control test results of Fig. 8, the contact friction is fully mobilized at a shear displacement of 0.35–0.4 mm, which coincides with the initiation of the shear dilation (Fig. 7b). This friction test result is plotted in Fig. 10 for each individual direct shear test. With given ϕ of 27° and measured D (or i) from Fig. 7b, shear strength component due to shear dilation was estimated from the direct shear tests using Eq. (1), and also included in Fig. 10 for each direct shear test. At the peak strength mobilization, the measured maximum shear dilation rate (D) values are 1.08, 0.79 and 0.42 for 3, 4.4 and 6 MPa direct shear tests, respectively. Assuming that the total shear strength observed in the direct shear test is the resultant of three components: (i) contact friction, (ii) shear dilation, and (iii) HCP–aggregate transition zone adhesion and cement–aggregate interlock. The strength due to adhesion and interlock can be estimated by subtracting the measured total strength from those of contact friction and shear dilation measured in the tests. This shear component derived from the adhesion and interlock before the peak strength was deduced for three direct shear tests, and included in Fig. 10, and re-plotted in Fig. 11 for comparison. From Fig. 10, both the friction and the cement–aggregate interaction including adhesion and interlock contribute a comparable effect on the strength mobilization up to the shear displacement of 0.35–0.4 mm. The cement–aggregate interaction probably involves formation and propagation of shear

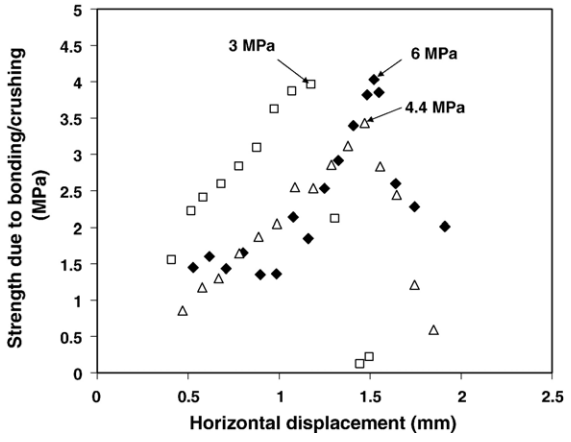

Fig. 11. Shear strength component due to HCP–aggregate transition zone adhesion as a function of shear displacement for direct shear tests at normal stresses of 3, 4.4 and 6 MPa.

Fig. 12. Shear crack dilation (direct shear test at 3 MPa).

cracks within the bulk HCP and in the vicinity of aggregate. After this stage, the material behaves non-linear. The friction remains constant with increasing shear displacement, and the shear dilation starts to play its role. The cement–aggregate interaction further enhances the total shear strength, reaches its maximum value of 3.4 to 4.2 MPa at a shear displacement of 1.2–1.5 mm, but starts to decline or vanish with further shearing (Fig. 11), which probably signifies the formation of a continuous sheared fracture across the specimen. At the peak, shear dilation is the major component contributing to the total strength, about 70%. After the peak, the shear dilation decreases drastically. The shear strength after the peak depends on the contact friction and post–peak dilation rate.

The cement–aggregate interlock may not exert a major influence on the total shear capacity observed in the three direct shear tests. This is because shear dilation or crack dilation was allowed in the tests. If the test specimen was restrained from vertical dilation or a very high normal confining stress was applied to the test specimen, cement–aggregate interlock would become activated. However, the sheared surface observed at the end of the direct shear tests (Figs. 12 and 13) clearly indicates that asperities of some aggregates (less than 10%) were sheared off and the surface had an average inclined angle of 8°, much

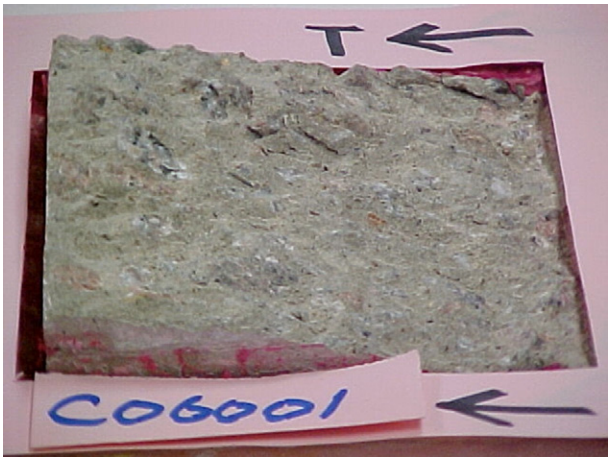

Fig. 13. Surface of sheared plane (direct shear test at 3 MPa).

less than the measured peak angle (i) of 30–46° in the direct shear tests. Local cement–aggregate interlock with aggregate crushing could be developed at local contact areas subjected to extremely high concentrated stresses. Thus, the shear strength component shown in Fig. 11 is probably dominated by the HCP–aggregate transition zone adhesion. This mobilized strength of 3.4–4.2 MPa is about 8–10% of the UCS, which is consistent with those observed by Sonnenberg et al. [14].

5. Discussion

5.1. Modes of failure

Three different types of tests, uniaxial compression, indirect tensile, and direct shear tests, were conducted in this study. Each type of test yields different mode of failure. The stress states at failure from three different types of tests are plotted in Fig. 14 for comparison. On this figure included are the non-linear and bi-linear envelopes proposed by Loov [7] and Sonnenberg et al. [14] based on push-off and direct tests results, respectively. It is important to note that in each type test the shear strength components are very different and their contribution may vary significantly in each case. This may explain the scatter in data if one determines failure envelope from test results from different types of tests without considering the mode of failure and type of shear strength component. For instance, a failure envelope encompassing Mohr's circles of UCS and indirect tensile test results will overestimate the strength under direct shear as shown in Fig. 14. Hence, it is critical to identify the correct mode of failure and use the appropriate failure envelope for design. In addition, strength mobilization could become the governing factor for serviceability state design.

It has been demonstrated that the shear capacity of concrete depends on adhesive strength of the HCP–aggregate transition zone, cement–aggregate interaction along the cracked surface, normal stress, and shear dilation. Fig. 14 shows the Mohr circle of a cylindrical concrete specimen at failure under uniaxial compression. The Mohr circle represents the possible stress states within the specimen. The normal stress variation within the specimen is wide, ranging from 0 to its ultimate compressive strength of about 40 MPa. The shear stress has a maximum value of about 20 MPa. The sheared or cracked sections

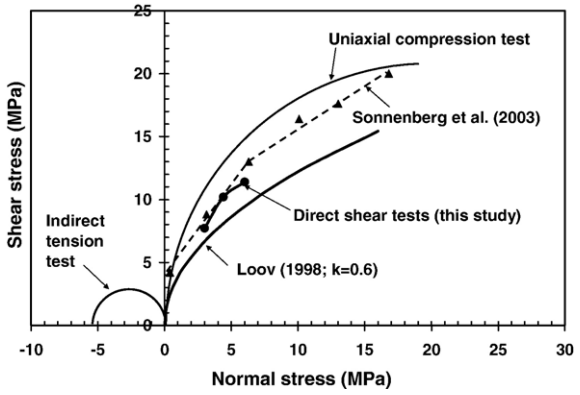

Fig. 14. Results of various strength tests in Mohr stress plot.

observed in the uniaxial compression tests are not planar, but conical developed at about 20 to 30° from the direction of the axial loading, which is probably due to the end restraint effect. The 3-D conical sheared surface provides a more stabilized effect than a planar surface, i.e., the compressive force required to cause sliding along the conical surface is greater than that along a plane [22]. This explains why the Mohr circle of the uniaxial compression test lies above the failure stress states of the direct shear tests. In addition, it is difficult to pin-point the exact failure stress state from the Mohr circle due to the ill-defined configuration of the cracked surface.

Brazilian test applies a line load to the concrete specimen which is stressed in biaxial tension and compression. Under this test condition, the stresses acting across the vertical diameter vary from high transverse compression at the top and bottom to a nearly uniform tension at two thirds mid-sections. This tensile stress at the mid-section causes the initial growth and interlinking of the micro-cracks within the HCP matrix and preexisting cracks in the transition zone between the HCP and aggregate. The concrete material fails in tensile splitting mode, and its Mohr circle is shown in Fig. 14. Since the failure mode in the splitting test is in pure tension, no shear stress would be induced along the crack. Relatively less energy is required for such tensile splitting than that in shear fracturing.

In the direct shear test, constant normal and shear forces are applied to the test specimen. For pre-cracked specimens, the normal and shear stress distributions across the crack surface are nearly uniform. However, for the initially uncracked specimens, the induced shear stress distribution across the sheared surface is complex and non-uniform, inducing principal stress rotation and thus roughened failure surface. However, the applied stresses still have a less variation in distribution as compared to those in the uniaxial compression tests. Thus, the shearing mode is well defined in direct shear tests. Direct shear test results on uncracked concrete specimen from this study and Sonnenberg et al. [14] are plotted in Fig. 14. The results are the applied shear and normal stresses values at the failure. The two concrete mixes have a close compressive strength of about 40 to 42 MPa. Both test series yield a very consistent trend in the shear failure envelope. Sonnenberg et al. [14] used a bi-linear failure envelope to interpret their test results. Based on their test results, we postulate that at low normal stress (<5–6 MPa), the shear stresses at the contact areas between the HCP and aggregates are not strong enough to cause crushing, and shear dilation (overriding) becomes dominant. At high normal stress (>5–6 MPa), the shear dilation is suppressed forming cement–aggregate interlock. Shear fracturing of the interlocked structure becomes a major contribution to the total shear capacity.

Fig. 14 also includes the shear friction failure envelope proposed by Loov [7]. Loov's correlation was derived from push-off tests on cracked reinforced concrete specimens. The normal stress was estimated based on the assumption that the steel reinforcement did reach its yield stress at failure. Also, the correlation does not consider the effect of the HCP–aggregate transition zone adhesion derived from the uncracked material on the shear capacity. This might explain why Loov's envelope lies below those determined from direct shear tests.

5.2. Shear reinforcement

Steel reinforcement for shear design in reinforced concrete members is assumed to reach its yield stress. One can use the results of direct shear tests to verify this important assumption. Consider the test results of the 6-MPa direct shear test (Fig. 7) as an illustrative example. The yield stress (f_y) and Young's modulus (E_s) of steel bars are assumed to be 345 MPa and 200 GPa, respectively. The normal confining stress of 6 MPa corresponds to a steel reinforcement ratio (ρ) of 1.74% where ρ is the ratio of steel reinforcement area to concrete area. Assuming that the tensile strain distribution along the embedded steel bar is a linear function increasing from zero at the end of its anchored length to the yield strain at the sheared or cracked section, the shear dilation (δ_v) in the sheared or cracked section required to induce yielding in steel bars is given by the following equation:

$$\delta_v = \left(\frac{f_y}{E_s}\right) L \tag{2}$$

where L = reinforcement anchorage length. For L = 305 mm, the shear interlocked dilation is equal to 0.53 mm. From Fig. 7b, the steel bars do reach its yield stress at the peak strength in this case. However, such a dilative crack may not be acceptable to serviceability.

6. Conclusion

Shear strength mobilization observed in direct shear tests on concrete specimens has been analyzed. The total shear strength comprises shear strength components derived from HCP–aggregate transition zone adhesion, contact friction, shear dilation, and cement–aggregate interlock along the sheared fractured surface. However, the behaviour in mobilization of each component varies and depends on the magnitude of shear displacement. Both HCP–aggregate transition zone adhesion and friction play a comparably important role in shear resistance at small shear displacement up to 0.4 mm. Shear displacement of about 0.4 mm is required to fully mobilize the contact friction, and the friction remains constant thereafter under constant normal stress. The HCP–aggregate transition zone adhesion (about 10% of unconfined compressive strength) becomes fully mobilized well before the peak strength, and decreases drastically. At the stage close to the peak, shear dilation becomes dominant contributing to about 70% of the total shear capacity. After the peak, cement–aggregate interlock could be developed at some local contact areas (less than 10%). Material brittle crushing along the rough sheared surface reduces the shear dilation resulting in a severe post–peak strength weakening. However, the cement–aggregate interlock mechanism was not dominant in the direct shear tests in this study because the specimen was allowed to dilate and the applied normal stress was not strong enough to suppress the dilation.

Acknowledgement

This study was made possible under collaboration between University of Calgary and Hong Kong Polytechnic University. Financial supports from NSERC and PolyU Project No. GT-213 are appreciated.

References

[1] ASCE-ACI committee 455, Recent approaches to shear design of structural concrete, Journal of Structural Engineering 124 (20) (1998) 1375–1417.
[2] R.E. Loov, A.K. Patnaik, Horizontal shear strength of composite concrete beams with a rough interface, PCI Journal 39 (1) (1994) 48–65.
[3] A.H. Mattock, Design proposals for reinforced concrete corbels, PCI Journal 25 (3) (1976) 18–25.
[4] J.C. Walraven, J. Frenay, A. Pruijssers, Influence of concrete strength and load history on the shear friction capacity of concrete members, PCI Journal 32 (1) (1987) 66–84.
[5] P.W. Birkeland, H.W. Birkeland, Connections in precast concrete construction, Journal of The American Concrete Institute 63 (3) (1966) 345–368.
[6] R.F. Mast, Auxiliary reinforcement in concrete connections, Journal of the Structural Division, ASCE 94 (ST6) (1968) 1485–1504.
[7] R.E. Loov, Review of A23.3-94 simplified method of shear design and comparison with results using shear friction, Canadian Journal of Civil Engineering 25 (1998) 437–450.
[8] P.K. Mehta, P.J.M. Monteiro, Concrete: structure, properties, and materials. Prentice Hall, Englewood Cliffs, New Jersey.
[9] J.A. Hofbeck, I.O. Ibrahim, A.H. Mattock, Shear transfer in reinforced concrete, Journal of the American Concrete Institute 66 (2) (1969) 119–128.
[10] T. Paulay, P. Loeber, Shear transfer by aggregate interlock, American Concrete Institute, Special Publication SP 42–1 (1974) 1–15.
[11] J.C. Walraven, Fundamental analysis of aggregate interlock, Journal of the Structural Division, ASCE 107 (ST11) (1981) 2245–2270.
[12] J.C. Walraven, H.W. Reinhardt, Theory and experiments on the mechanical behaviour of cracks in plain and reinforced concrete subjected to shear loading, Heron 26 (1A) (1981) 1–68.
[13] J.C. Walraven, J. Stroband, Shear friction in high strength concrete, ACI International Conference on High Performance Concrete SP-149 (1994) 311–330.
[14] A.M.C. Sonnenberg, R. Al-Mahaidi, G. Taplin, Behaviour of concrete under shear and normal stresses, Magazine of Concrete Research 55 (4) (2003) 55–65.
[15] M.W. Braestrup, Plastic analysis of shear in reinforced concrete, Magazine of Concrete Research 26 (89) (1974) 221–228.
[16] M.P. Nielsen, Limit analysis and concrete plasticity, Prentice-Hall Inc, Englewood Cliffs, N.J., 1984.
[17] J.P. Zhang, Diagonal cracking and shear strength of reinforced concrete beams, Magazine of Concrete Research 49 (178) (1997) 55–65.
[18] ASTM, Volume 04.02 concrete and aggregates, American Society for Testing and Materials, 1998.
[19] S.A. Mirza, M. Hatzinikolas, J.G. MacGregor, Statistical descriptions of the strength of concrete, Journal of the Structural Division, ASCE 105 (ST6) (1979) 1021–1037.
[20] J.G. MacGregor, F.M. Bartlett, Reinforced Concrete: Mechanics and Design, 1st Canadian edition, Prentice Hall Canada Inc., Scarborough, Ontario, Canada, 2002.
[21] P.W. Rowe, The stress-dilatancy relation for static equilibrium of an assembly of particles in contacts, Proceedings, Royal Society of London 269 (1962) 500–527.
[22] R.C.K. Wong, Mobilized strength components of oil sand in triaxial compression, Canadian Geotechnical Journal 36 (2000) 718–735.